Journal of Inorganic and Organometallic Polymers and Materials (2025) 35:7110–7128
https://doi.org/10.1007/s10904-025-03772-x

RESEARCH

# Construction of Nickel Hydroxide Based Electrode Material and Its Performance for Non-enzymatic Glucose Sensing Applications

**Cigdem Dulgerbaki**[1]

Received: 1 November 2024 / Accepted: 3 April 2025 / Published online: 25 April 2025


**Abstract**
Conventional nanomaterials are used in electrochemical glucose non-enzymatic sensing, but their widespread application is restricted by high costs and complex preparation procedures. This study explores the use of nickel hydroxide ($Ni(OH)_2$), which was deposited onto the entire surface of a screen-printed gold electrode (SPGE) through one-step electrodeposition process, serving as an interface material for non-enzymatic glucose sensing. The surface morphology, composition and electrochemical properties of SPGE/$Ni(OH)_2$ were investigated using scanning electron microscopy (SEM), energy-dispersive X-ray spectroscopy (EDX), elemental mapping, cyclic voltammetry (CV) and chronoamperometry (CA). CV and CA results revealed that SPGE/$Ni(OH)_2$ exhibited excellent electrocatalytic activity towards glucose. The oxidation current was directly proportional to glucose concentrations ranging from 10 µM to 200 µM. Furthermore, the glucose sensor demonstrated a low detection limit of 1.8 µM in a basic solution and exhibited excellent selectivity. With its facile preparation and reliable performance, this sensor is a promising candidate for the next generation non-enzymatic glucose diagnostic devices.

**Keywords** Nickel hydroxide · Non-enzymatic sensor · Glucose detection · Electrodeposition · Screen printed gold electrode

## 1 Introduction

Glucose is a vital nutrient in the human body, serving as a key energy source for biological metabolism. However, abnormal glucose concentrations in the blood can lead to acute conditions such as diabetes, obesity and hypertension, which impose a significant financial burden and reduce quality of life [1]. If these conditions are not adequately managed, they can cause complications that pose serious threats to human health. Therefore, the rapid and accurate measurement of blood glucose levels is crucial for preventing and controlling these diseases [2]. Additionally, effective glucose detection is important in the food industry, pharmaceutical manufacturing, environmental monitoring and other fields [3]. Consequently, there is a high demand for cost-effective, rapid and reliable methods for quantitatively determining glucose concentration, driving ongoing industry interest in developing new sensors for clinical diagnostics, food industry and biotechnology [4].

Significant efforts have been dedicated to developing sensitive, selective and reliable methods for detecting blood glucose. Techniques such as colorimetry, optical methods, electrochemiluminescence and fluorescent spectroscopy have been explored, but electrochemical sensors have garnered considerable attention due to their simplicity, low cost, high sensitivity, straightforward instrumentation, easy operation and ease of integration [5]. Currently, most commercially available glucose biosensors are based on the catalytic activity of an immobilized enzyme, which provides high sensitivity and satisfactory selectivity. However, these enzyme-based glucose sensors often face issues of instability, high production costs and complex immobilization procedures, which can be adversely affected by environmental conditions. Therefore, the development of electrochemical non-enzymatic glucose sensors, which typically rely on the direct oxidation of glucose molecules, is essential and

✉ Cigdem Dulgerbaki
cigdem.dulgerbaki@alanya.edu.tr

[1] Faculty of Engineering, Department of Engineering Fundamental Sciences, Alanya Alaaddin Keykubat University, Alanya, Antalya, Turkey

regarded as the most effective and advantageous approach for glucose detection [6–8].

Extensive research has been conducted on non-enzymatic glucose sensors utilizing transition metal and metal oxide nanomaterials [9]. Metal oxides or hydroxides, such as $MnO_2$ [10], CuO [11], $Co_3O_4$ [12] and $Ni(OH)_2$ [13] are commonly used as catalytic materials in these sensors. Among these, $Ni(OH)_2$, a non-noble transition metal hydroxide, has demonstrated excellent electrocatalytic activity for glucose in alkaline media. This is attributed to its good anti-interference properties, excellent electrochemical stability, environmental friendliness and low cost. The enzymatic-free oxidation of glucose is significantly enhanced by the $Ni(OH)_2$/NiOOH redox couple formed on the electrode surface [14]. Consequently, various synthesis methods have been employed to prepare $Ni(OH)_2$-based modified electrodes for glucose detection, including solution-based synthesis [15], pulsed laser deposition [16], sol–gel synthesis [17] and electrodeposition [18].

Microfabricated electrodes offer a significant advantage over traditional electrodes in electrochemical sensing by paving the way for the development of highly reproducible, precise and sensitive sensors. Among these, screen-printed electrodes (SPEs) have gained widespread application in chemical and biological detection due to their affordability, ease of fabrication, rapid production and versatility. They can be manufactured from various materials with adaptable selectivity, require only small sample volumes of analyte and generate minimal waste. Consequently, they eliminate common challenges associated with conventional solid electrodes, such as surface contamination, passivation and tedious cleaning procedures [19]. Glucose sensors utilizing SPEs have recently attracted considerable interest due to their low cost, ease of use for on-site analysis and ability to be modified with various materials while requiring only small sample volumes [20]. Additionally, SPEs offer rapid response times with high sensitivity and selectivity [21] making them well-suited for integration into portable [22] and wearable sensors [23] for clinical diagnostics and personal healthcare monitoring. Various materials and technologies have been developed to enhance the efficiency and performance of SPEs, incorporating different materials such as carbon, mercury, bismuth and gold. Among these, the screen-printed gold electrode (SPGE) has emerged as a promising alternative to conventional carbon electrodes, driven by advancements in printed electrode production technologies. Typically, the SPGE consists of gold working electrode, gold counter electrode and silver reference electrode, all printed on a ceramic substrate. Compared to traditional electrodes, SPGEs represent a significant innovation due to their fabrication via mass production techniques. They are user-friendly and often designed for single-use applications. Furthermore, SPGEs offer excellent reproducibility in electrochemical analysis, making them highly valuable for various sensing applications and electrochemical platforms [24].

The motivation of the present work is to construct Ni$(OH)_2$ nanoparticle modified SPGE and the study of its electrochemical applicability in non-enzymatic voltammetric and amperometric detection of glucose. A facile and cost-effective technique with excellent electrochemical activity toward glucose has been implemented which is as effective as sophisticated sensors. The electrochemical performance of SPGE/$Ni(OH)_2$ was investigated by using CV and CA techniques. The SPGE/$Ni(OH)_2$ sensor is capable of selectively detecting glucose even in the presence of potential interfering agents such as ascorbic acid, fructose and maltose. Its hierarchical nanostructure provides a high surface area and facilitates easy permeability for the diffusion and electron transfer of glucose, resulting in enhanced sensing performance.

The $Ni(OH)_2$ is a promising electrocatalyst in electrochemical glucose biosensing applications. However, to the best of our knowledge, there are no reports in the literature on the use of electrochemically deposited SPGE/$Ni(OH)_2$ based material that can boost the electrocatalytic activity of non-enzymatic glucose sensing. In this paper, as far as we know, SPGE/$Ni(OH)_2$ was first applied to the non-enzymatic glucose sensor in order to achieve the detection of glucose by using low-cost materials and energy-saving methods. SPGE/$Ni(OH)_2$ was prepared by directly depositing the nickel hydroxide on a SPGE with a facile electrochemical method. Moreover, the electrodeposition method has made a great contribution to the uniform and strong loading of $Ni(OH)_2$ on the SPGE substrate, which is beneficial to the detection performance of the SPGE/$Ni(OH)_2$ for glucose. The modification of SPGE with $Ni(OH)_2$ by electrodeposition is beneficial to enlarge its active surface area and improve its electrocatalytic performance. Therefore, this study explores the possibility of employing SPGE/$Ni(OH)_2$ for non-enzymatic electrochemical glucose sensing.

## 2 Experimental

### 2.1 Materials

The materials used in this research, nickel acetate, sodium hydroxide, glucose, ascorbic acid, fructose and maltose were sourced from Sigma-Aldrich Corp. (USA) and met analytical grade standards. Alkaline solutions were prepared with NaOH pellets and all solutions were made using deionized water. The experiments were carried out at standard

room temperature. SPGEs were procured from Metrohm DropSens S.L. (Spain).

### 2.2 Construction of the $Ni(OH)_2$ Non-enzymatic Glucose Sensor

$Ni(OH)_2$ was deposited onto the SPGE using a potentiostatic method [25]. 0.1 M nickel acetate ($Ni(CH_3COO)_2{\cdot}4H_2O$) solution was freshly prepared for this deposition. Twenty microliters (20 µL) of this solution was applied to the SPGE and the electrodeposition was carried out at a constant potential of -0.9 V for 800 s. For glucose detection, solutions with concentrations from 1 mM to 10 mM and 10 µM to 200 µM were prepared in 0.1 M NaOH. As the glucose concentration increased, the anodic peak current at approximately + 0.7 V also increased, reflecting the interaction between glucose and $Ni(OH)_2$ in the alkaline medium. To use the $Ni(OH)_2$ sensor, 20 µL of glucose solution in 0.1 M NaOH was drop-casted onto the electrode. After a 10-second resting period for hydroxide ions to facilitate $Ni(OH)_2$ oxidation, CV was conducted over a potential range of − 1.0 V to + 1.0 V and CA was conducted at + 0.63 V for 1200 s.

### 2.3 Instrumentation

Electrochemical measurements were conducted using a Metrohm Dropsens µStat-i potentiostat/galvanostat, paired with SPGEs sourced from Metrohm DropSens in Spain. These electrodes formed a 3-electrode system comprising gold working and counter electrodes, a silver quasi-reference electrode and electrical contacts. The working electrode featured a diameter of 4 mm. A DRP-DSC connector was used to link the SPGEs to the potentiostat. CV experiments were performed at a scan rate of 100 mV/s over a potential range of − 1.0 V to + 1.0 V to assess the electrochemical characteristics of each sample. To analyze the morphology of $Ni(OH)_2$-modified electrodes, a LS10 scanning electron microscope from Zeiss Evo, Carl Zeiss NTS (Germany) was employed, equipped with an energy-dispersive X-ray spectroscopy detector for elemental analysis.

## 3 Results and Discussion

SEM images of SPGE/$Ni(OH)_2$ at varying magnifications (1 µm and 200 nm) are illustrated in Fig. 1a and b, respectively. Both figures reveal the agglomerated, rock-like nanostructures of $Ni(OH)_2$, which exhibit a rigid surface morphology with a dispersed nature. Generally, nickel

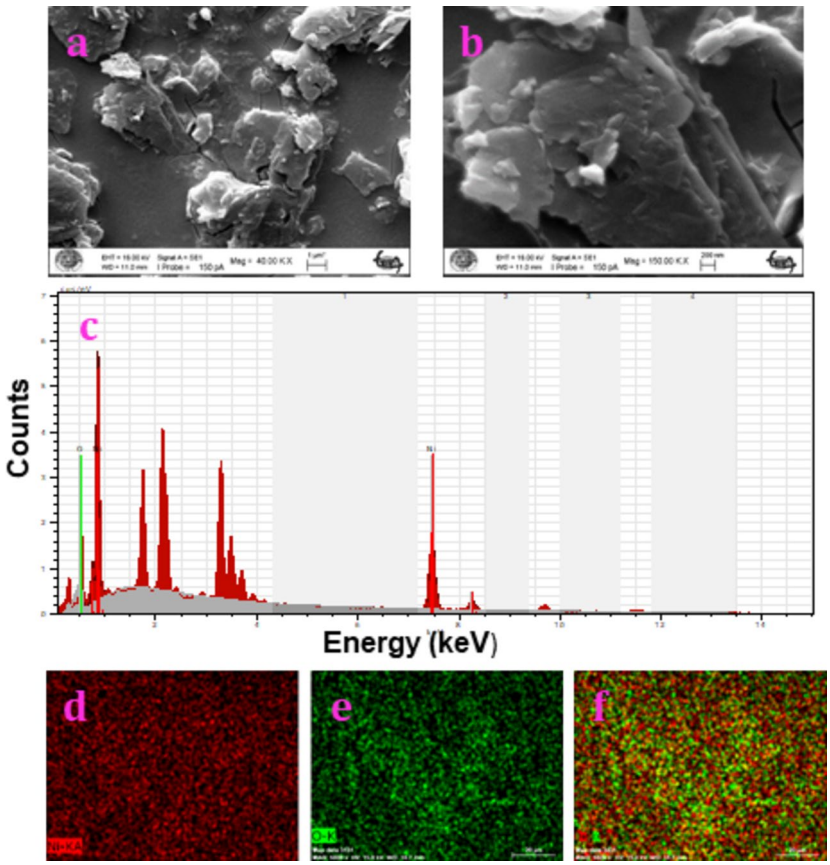


**Fig. 1** **a** SEM image of SPGE/$Ni(OH)_2$ at 1 µm **b** SEM image of SPGE/$Ni(OH)_2$ at 200 nm **c** EDX spectrum of $Ni(OH)_2$**d**–**f**) Elemental mapping of $Ni(OH)_2$**d** nickel (red) **e** oxygen (green) **f** overall mapping

hydroxide with irregular shape possess a higher specific surface area which can provide a high density of active sites and accordingly promote intimate interaction between the active material and the surrounding electrolyte [26]. This morphology is advantageous for enhancing electron transport pathways, thereby improving the glucose oxidation reaction.

Elemental analysis using EDX and elemental mapping confirmed the chemical composition of $Ni(OH)_2$, identifying nickel (Ni) and oxygen (O) as its primary elements. These elements are clearly represented in the EDX spectrum of $Ni(OH)_2$ (Fig. 1c), with Ni and O percentages measured at 12.62% and 87.38%, respectively. The uniform distribution of Ni and O on the $Ni(OH)_2$ electrode's surface is depicted in Figs. 1(d–f) through elemental mapping images, where red and green colors correspond to Ni and O, respectively.

### 3.1 Voltammetric Characteristics of SPGE/$Ni(OH)_2$ Towards Glucose

Cyclic voltammetry (CV) is a valuable and practical technique for observing electron transfer processes at modified electrodes. This method was used to evaluate the electrocatalytic activity and non-enzymatic glucose sensing capabilities of electrodes in an alkaline medium. Figure 2 shows the CV responses of the bare SPGE and the SPGE/$(NiOH)_2$ electrode in the absence and presence of glucose.

The bare SPGE displays no distinct oxidation or reduction peaks, indicating limited electrochemical reactivity. In contrast, the SPGE/$(NiOH)_2$ electrode exhibits clear anodic and cathodic peaks at +0.12 V and −0.25 V, respectively, which are associated with the Ni(II)/Ni(III) redox couple [27]. When glucose is added, the oxidation peak becomes more pronounced while the reduction peak diminishes, suggesting that $Ni(OH)_2$ effectively catalyzes glucose oxidation in the NaOH solution. This result is consistent with previous studies on glucose detection using NiO-based materials [28]. Furthermore, the anodic peak potential shifts to a

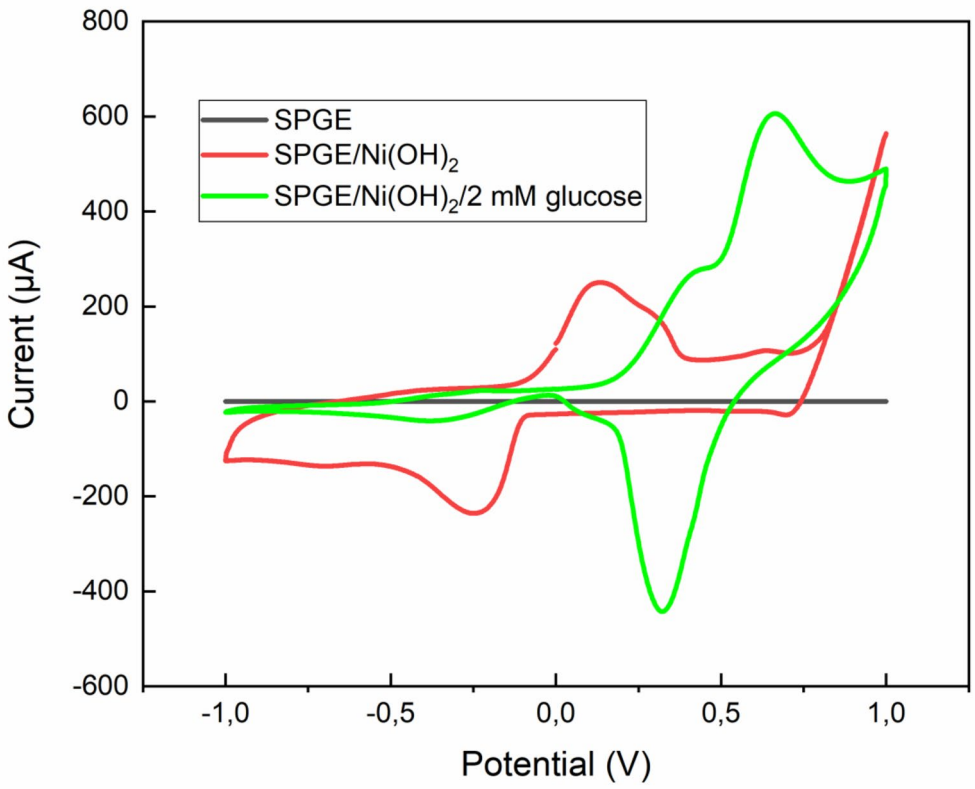


**Fig. 2** CV curves of SPGE and $Ni(OH)_2$ modified SPGEs before and after addition of 2 mM glucose in 0.1 M NaOH solution at the scan rate of 100 mV $s^{-1}$

higher value, likely due to glucose diffusion limitations at the electrode surface.

The glucose oxidation mechanism facilitated by NiO-based materials can be outlined by the following reactions:

$$Ni(OH)_2 + OH^- \rightarrow NiOOH + H_2O + e^- \quad (1)$$

$$NiOOH + \text{glucose} \rightarrow Ni(OH)_2 + \text{gluconolactone} \quad (2)$$

In the CV forward scanning process, the $Ni(OH)_2$ grown on the SPGE surface is electrochemically oxidized to NiOOH in 0.1 M NaOH solution (Eq. (1)). Owing to the transformation of electrons, the anodic current peak is formed simultaneously. Based on Eq. (2), NiOOH then involves in the oxidation of glucose ($C_6H_{12}O_6$), which generates gluconolactone ($C_6H_{10}O_6$) and $Ni(OH)_2$. With this reaction, the cathodic current peak is much lower than the anodic current peak because the electrons released by glucose oxidation do not pass through the electrode (Fig. 2) [29].

The anodic peak reflects the electron release associated with the oxidation of Ni(II) hydroxide (Ni(II)$(OH)_2$) to nickel oxy-hydroxide (Ni(III)OOH). The cathodic peak corresponds to the reversible reduction of Ni(III)OOH back to Ni(II) hydroxide in alkaline media [7]. Upon adding 2 mM glucose, significant changes are observed in both the anodic and cathodic currents, indicating the electrooxidation of glucose to gluconolactone by Ni(III)OOH (Eq. (2)). Simultaneously, Ni(III)OOH is reduced back to Ni(II) $(OH)_2$, demonstrating effective electrochemical catalysis of glucose oxidation by the modified electrodes. Additionally, both the cathodic and anodic peak potentials shift positively, which is attributed to glucose diffusion limitations during the catalytic process [13].

Figure 3 represents the CVs of the SPGE/$Ni(OH)_2$ electrode in 0.1 M NaOH solution at various scan rates. The data reveal a clear increase in both anodic and cathodic peak currents with rising scan rates. The inset graph illustrates a linear relationship between the anodic peak current and the square root of scan rate over the range of 25–100 mV/s, with a correlation coefficient of $R^2 = 0.9973$. This linearity suggests that the electrooxidation of glucose follows a diffusion-controlled electrochemical process, which is

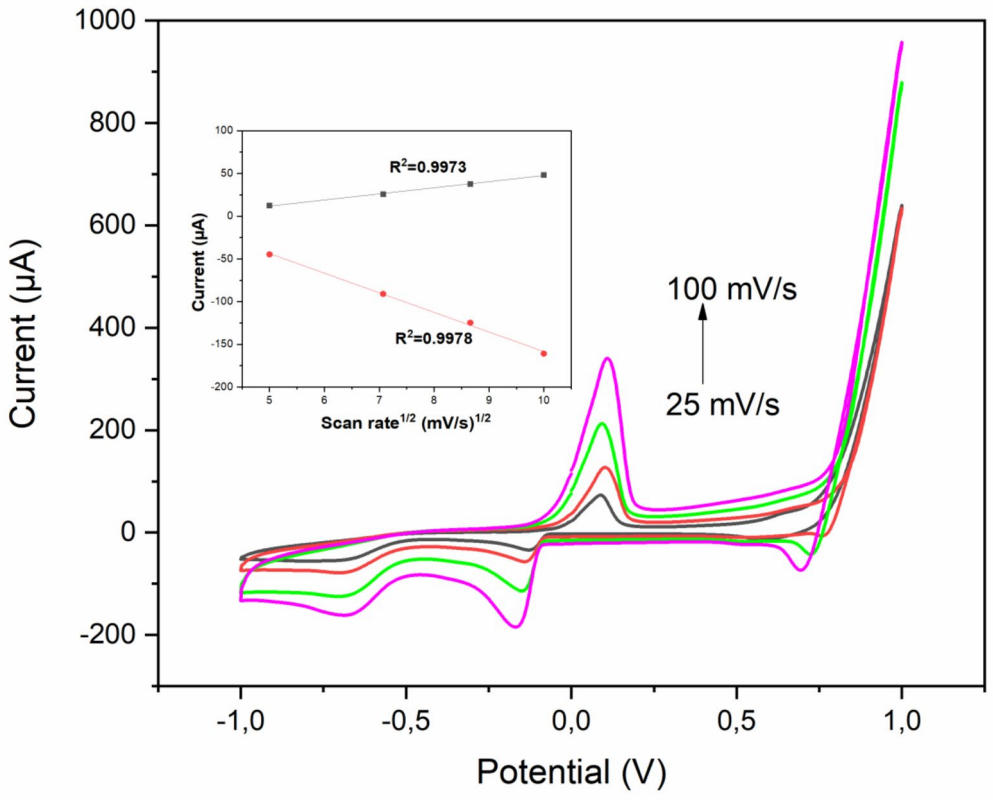


**Fig. 3** CVs of the SPGE/$Ni(OH)_2$ in 0.1 M NaOH with different scan rates. Inset: the relationship between cathodic and anodic peak current with the scan rate

advantageous for quantitative analysis in practical applications [30].

Figure 4 presents the CV curves of the SPGE/Ni(OH)₂ electrode in 0.1 M NaOH solution with varying glucose concentrations, ranging from 1 mM to 10 mM, measured at a scan rate of 100 mV/s. As glucose is progressively added, there is a significant increase in the anodic peak current (Ipa), which indicates effective oxidation of the glucose molecules. This substantial rise in Ipa highlights the excellent electrocatalytic performance of the SPGE/Ni(OH)₂ electrode, attributed to the superior catalytic properties of Ni(OH)₂. The linear and noticeable increase in Ipa at an applied potential of approximately + 0.63 V suggests that the SPGE/Ni(OH)₂ electrode is highly sensitive and demonstrates excellent linearity, making it a promising candidate for glucose sensing applications [31].

In Fig. 4, the CV curves for the SPGE/$Ni(OH)_2$ electrode show that with increasing glucose concentration, the anodic peak currents progressively increase, while the cathodic peak currents decrease. Additionally, the oxidation peak shifts slightly to higher potentials with higher glucose concentrations in 0.1 M NaOH. This shift is attributed to the greater energy required for glucose diffusion on the electrode surface at higher concentrations [32]. These observations confirm that the SPGE/Ni(OH)₂ electrode demonstrates excellent catalytic performance for glucose oxidation.

Figure 5 illustrates the calibration curve for the SPGE/$Ni(OH)_2$ glucose sensor. The sensor demonstrates an increased response with rising glucose concentrations, showing a reliable linear range from 1 mM to 10 mM glucose. The linear regression equation, I(μA) = 240.122c(mM) + 133.053 with a correlation coefficient ($R^2$) of 0.9924, reflects a strong linear relationship within this range [33].

In practical scenarios, other organic species present in human blood can potentially interfere with the non-enzymatic electrooxidation of glucose [34]. Therefore, evaluating the specificity and selectivity of the working electrode is essential and must be confirmed through interference testing. Figure 6 displays the cyclic voltammetric response of the SPGE/$Ni(OH)_2$ electrode when 1 mM ascorbic acid,

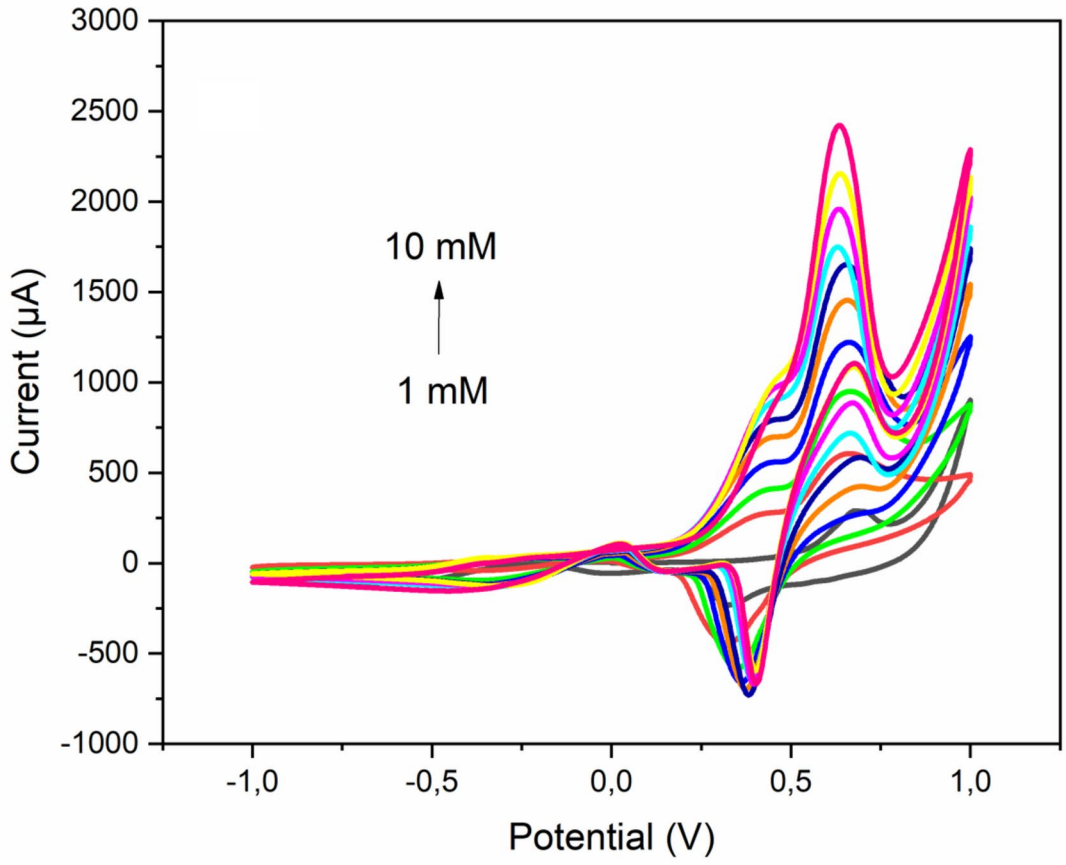


**Fig. 4** CV curves of $Ni(OH)_2$ modified SPGE under various glucose concentration from 1 mM to 10 mM in 0.1 M NaOH solution

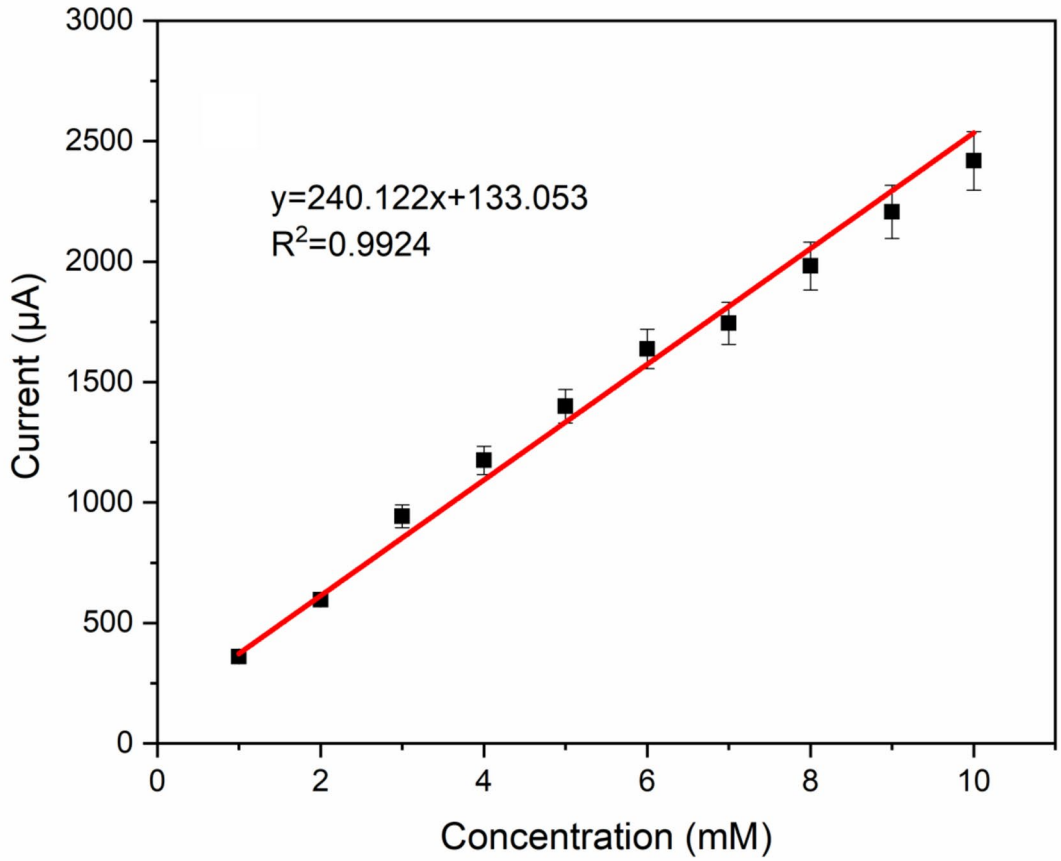


**Fig. 5** Calibration plot between the anodic peak currents vs. glucose concentration

fructose and maltose are added to glucose solutions. The results indicate that these interfering substances produce no significant current response compared to glucose in 0.1 M NaOH solution. Additionally, a comparative bar chart in Fig. 7 provides a clear overview of the negligible current increase caused by these interfering species, demonstrating that they do not impact glucose electrooxidation on the SPGE/Ni(OH)$_2$ electrode. These findings confirm that the SPGE/Ni(OH)$_2$ electrode exhibits acceptable selectivity for glucose detection.

### 3.2 Amperometric Characteristics of SPGE/Ni(OH)$_2$ Towards Glucose

The analytical performance of the sensor was evaluated by examining its reproducibility, sensitivity, selectivity and stability. Among these parameters, reproducibility is particularly critical for assessing both the sensor's performance and the consistency of the manufacturing process. To evaluate reproducibility, five sensors were tested by conducting chronoamperometry (CA) measurements in 0.1 M NaOH (Fig. 8). The relative standard deviation (RSD) of the sensor responses was calculated to be 3.09%, which falls within the acceptable range for biosensing applications [35].

To evaluate sensor performance, glucose concentrations ranging from 0.01 mM to 0.2 mM were sequentially introduced into 20 mL of stirred 0.1 M NaOH after every 100 s while maintaining a constant applied potential of + 0.63 V, as shown in Fig. 9. Following each glucose injection, the modified electrode exhibited a rapid stepwise increase in current response, reaching a steady state within 3 s. This fast stabilization suggests efficient electron transfer kinetics, consistent with the CV results. The steady-state current increased with higher glucose concentrations, attributed to glucose oxidation and the formation of hydrogen peroxide ($H_2O_2$) at the sensor surface [36]. The corresponding calibration plot for the CA measurements, shown in Fig. 10, illustrates a linear response to glucose concentrations between

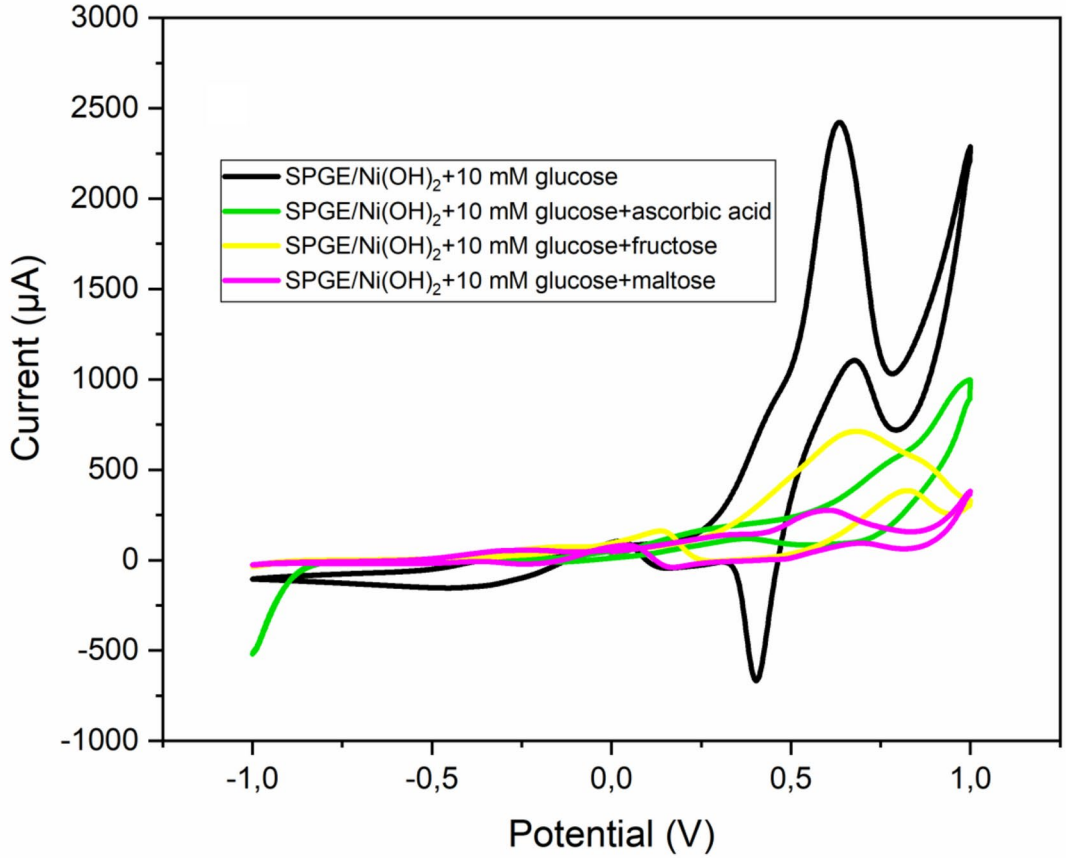


**Fig. 6** The impact of biomolecules on interference

10 µM and 200 µM. However, at higher concentrations, the response deviated from linearity, likely due to sensor surface saturation and glucose accumulation [37].

Figure 10 presents the calibration curve for the chronoamperometric current response of SPGE/$Ni(OH)_2$ to glucose, demonstrating a linear relationship between the oxidation current and glucose concentration within the range of 0.01 mM to 0.2 mM. Glucose analysis within this linear range (10–200 µM) exhibited a high correlation coefficient ($R^2$ = 0.9914) and remarkable sensitivity (10.202 µA $\mu M^{-1}$ $cm^{-2}$), as determined from the linear equation I(µA) = 10.202c(µM) + 393.283. Furthermore, the limit of detection (LOD) for glucose in this study was calculated as 1.8 µM using the formula: LOD = 3.3 × (standard deviation of the regression line (σ)) / slope (S). These findings underscore the outstanding performance of the proposed sensor as a highly sensitive and non-enzymatic electrochemical glucose sensor.

Selectivity is a crucial factor in evaluating the analytical performance of non-enzymatic glucose sensors. To assess the selectivity of the sensor and potential interference from other substances, ascorbic acid, fructose and maltose were tested. These substances typically exist in biological samples at concentrations ranging from 0.1 to 0.2 times that of glucose [38]. In this study, anti-interference ability of the sensor was evaluated by adding 10 µM glucose to 0.1 M NaOH, followed by the sequential introduction of interfering substances at their physiological concentrations of 1 µM at specific intervals, as shown in Fig. 11. The oxidation current response of glucose remained dominant, while the signals from interfering agents were minimal, demonstrating the high selectivity of the sensor for glucose oxidation at a fixed potential of + 0.63 V.

One of the key advantages of non-enzymatic sensors is their high stability at room temperature compared to enzymatic biosensors [36, 38]. To evaluate the stability of the proposed sensor, its chronoamperometric response was

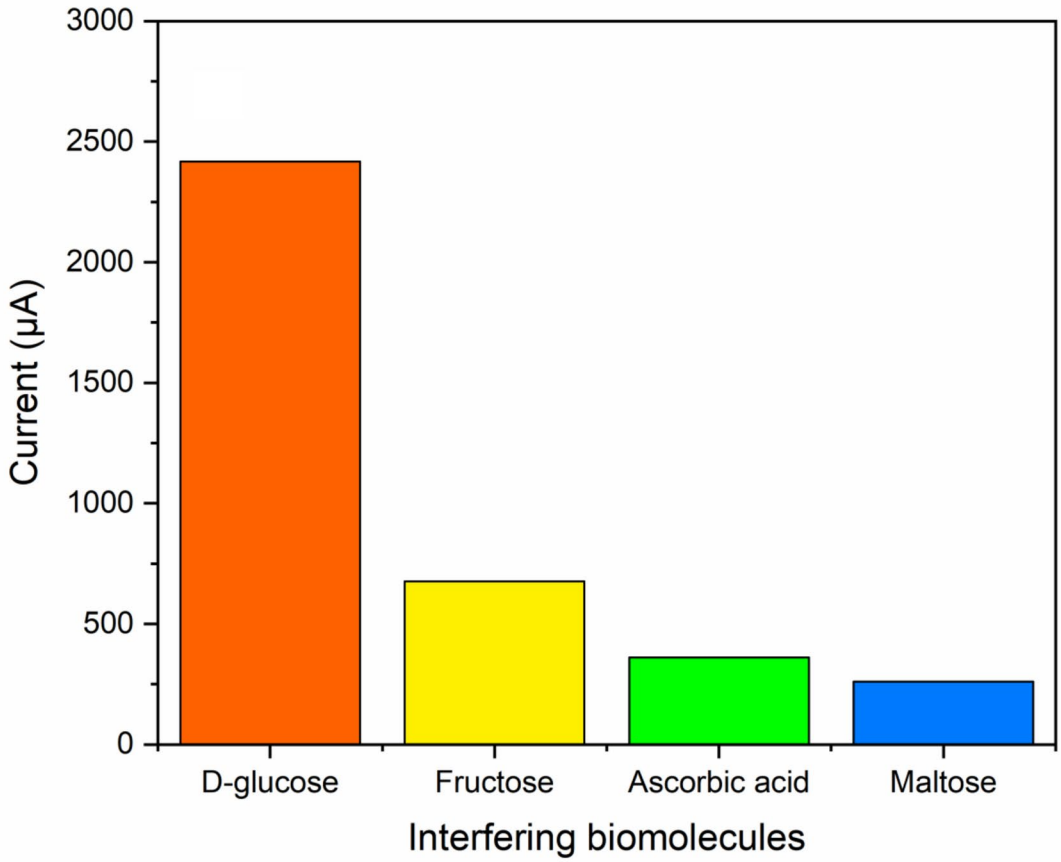


**Fig. 7** Bar graph depicting the interference effect

measured in the presence of 100 μM glucose in 0.1 M NaOH, as shown in Fig. 12. After a storage period of two months, the current response of the electrode for glucose oxidation was re-measured. Remarkably, the SPGE/$Ni(OH)_2$ electrode retained approximately 93% of its initial current response, demonstrating excellent long-term stability. The amperometric response of the electrode after two months was nearly identical to its performance prior to storage. These findings highlight the superior stability of the developed sensor at room temperature, outperforming many previously reported sensors [37].

In order to validate the commercial reliability and practical applicability of the SPGE/$Ni(OH)_2$ electrode as a glucose sensor, glucose concentrations in real samples were analyzed using the amperometric method. The sensor's response to glucose oxidation was tested with commercially available fluids, including apricot juice, sourcherry juice, orange juice, coke and sprite, as shown in Fig. 13. A fluid solution containing 3 mM glucose was prepared for sensing purposes, following a previously reported method [39]. Specifically, 1 mL of each fluid (3 mM) was dissolved in 30 mL of 0.1 M NaOH and the amperometric response was measured at the applied potential for each sample. Among the tested samples, coke exhibited the highest current response compared to the other fluids as shown in Fig. 14. Table 1 summarizes the sugar content of each fluid and the corresponding current response observed during the sensing tests. These findings demonstrate that the prepared SPGE/$Ni(OH)_2$ electrode is capable of selectively detecting glucose in real samples, underscoring its potential for practical applications.

To assess the synthesized electrode for non-enzyme glucose sensors, a comparison with other reported electrodes is summarized in Table 2. The SPGE/$Ni(OH)_2$ electrode demonstrates exceptional glucose electrocatalytic activity, including a broader linear range and a lower detection limit. Our approach offers a straightforward and cost-effective method for electrodepositing $Ni(OH)_2$ onto the SPGE

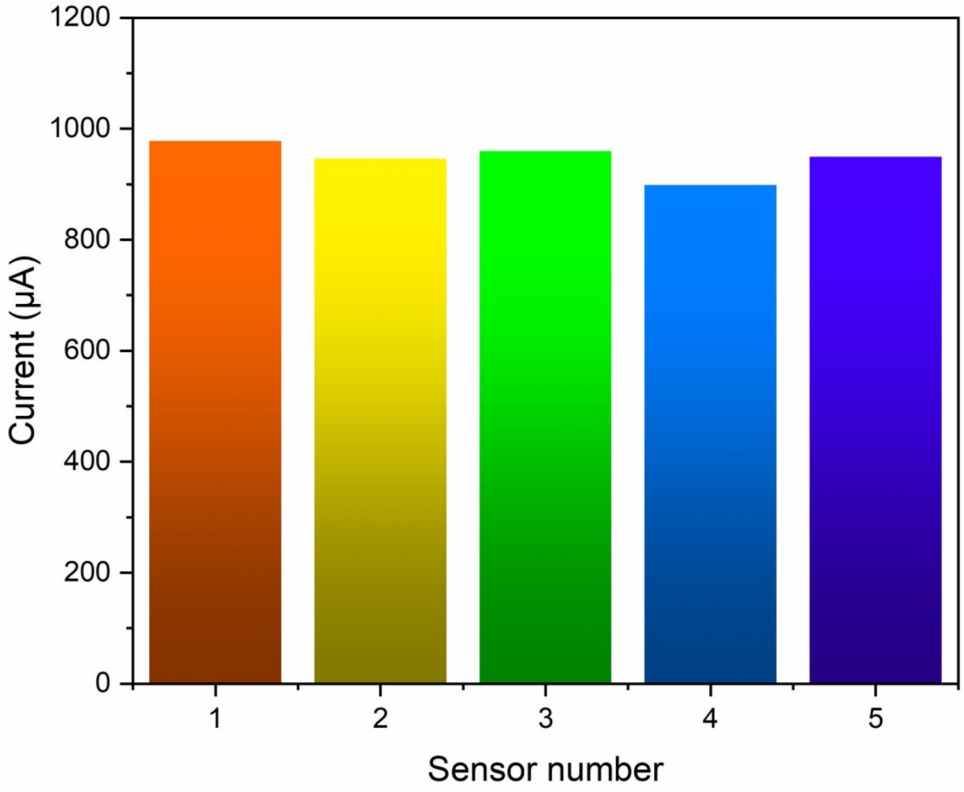


**Fig. 8** Reproducibility results for chronoamperometry of different sensors in 0.1 M NaOH

network, avoiding the use of high temperatures, toxic nickel salts and binders.

## 4 Conclusion

This study introduces a practical and cost-effective one-step method for synthesizing SPGE/$Ni(OH)_2$ for use in electrochemical glucose sensors, eliminating the need for complex modifications and assemblies. Electrochemical investigations reveal that the material exhibits excellent catalytic activity for the enzyme-free electrooxidation of glucose in alkaline conditions. Electrocatalytic performance metrics show that SPGE/$Ni(OH)_2$ has a broad linear range extending up to 200 μM, a detection limit as low as 1.8 μM and can selectively identify glucose even in the presence of interfering substances. The improved electrocatalytic performance is attributed to efficient electron transfer and abundant active sites within the material. Given its facile preparation process and superior electrocatalytic properties, this approach offers a valuable framework for developing metal hydroxide-based materials for non-enzymatic electrochemical sensing.

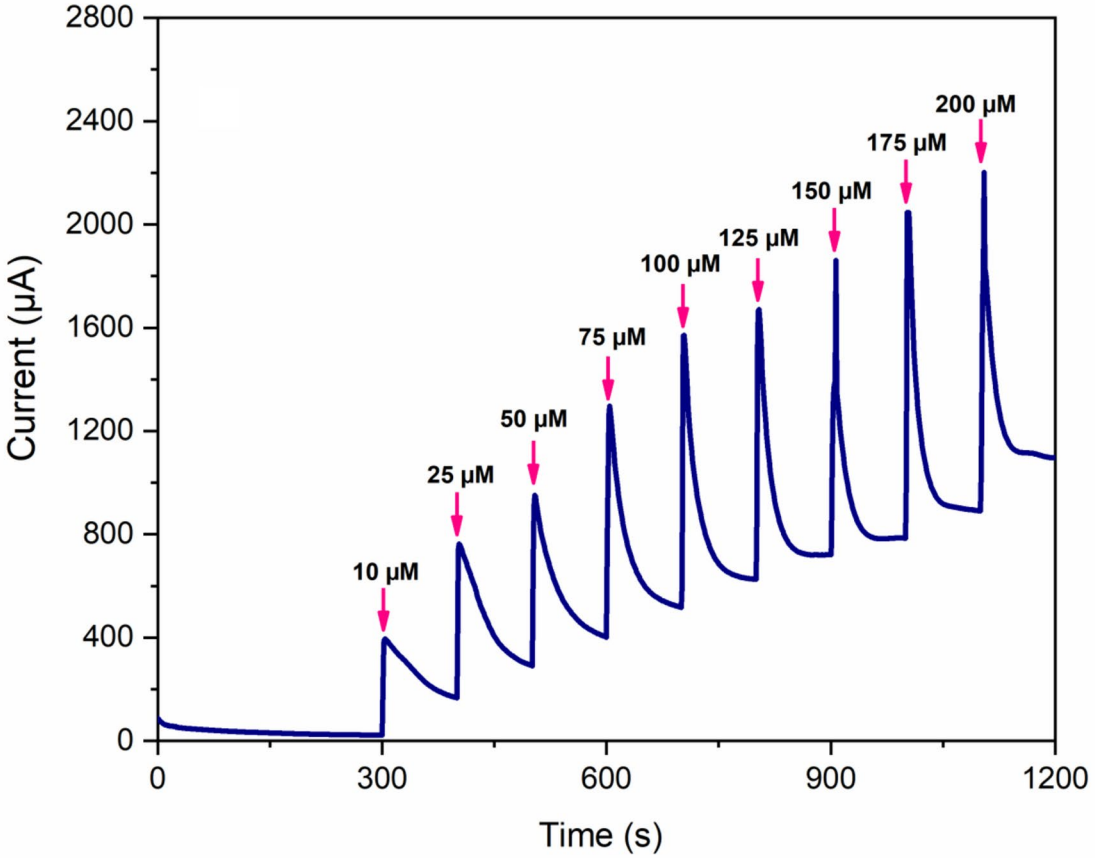


**Fig. 9** Amperometric response of SPGE/$Ni(OH)_2$ with step-wise glucose addition in 0.1 M NaOH at a fixed potential of + 0.63 V

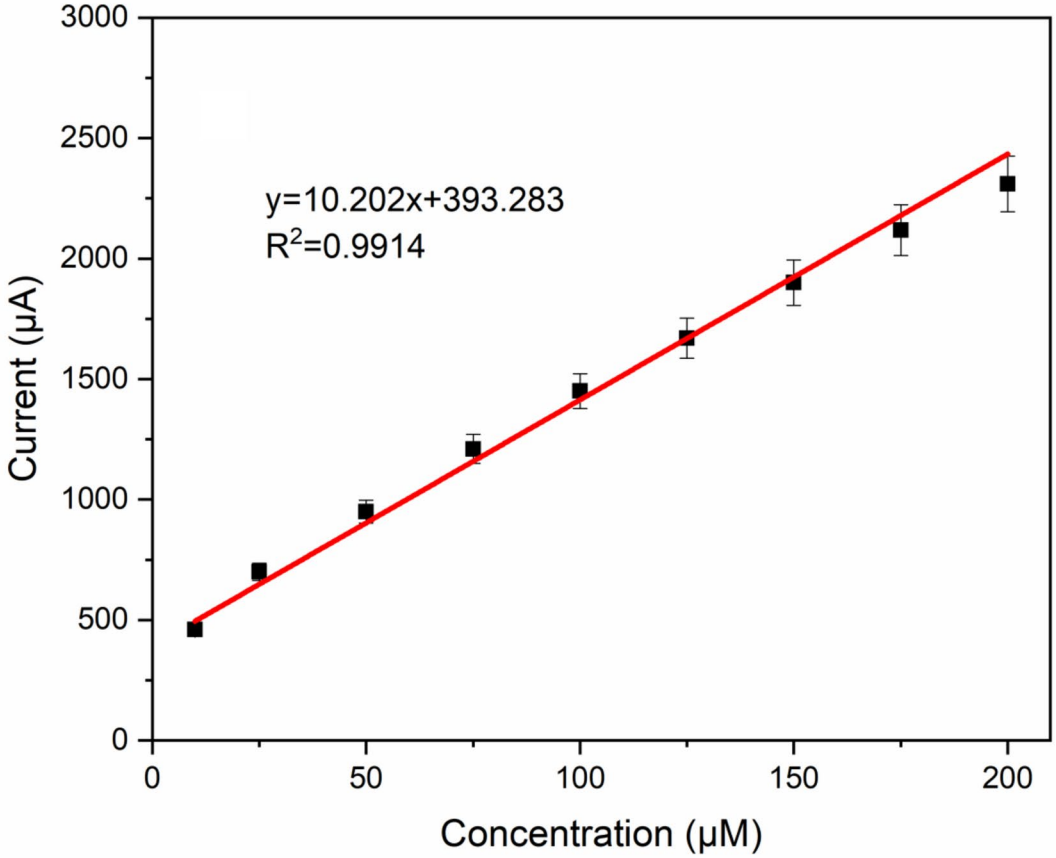


**Fig. 10** Calibration plot of glucose concentration and response current

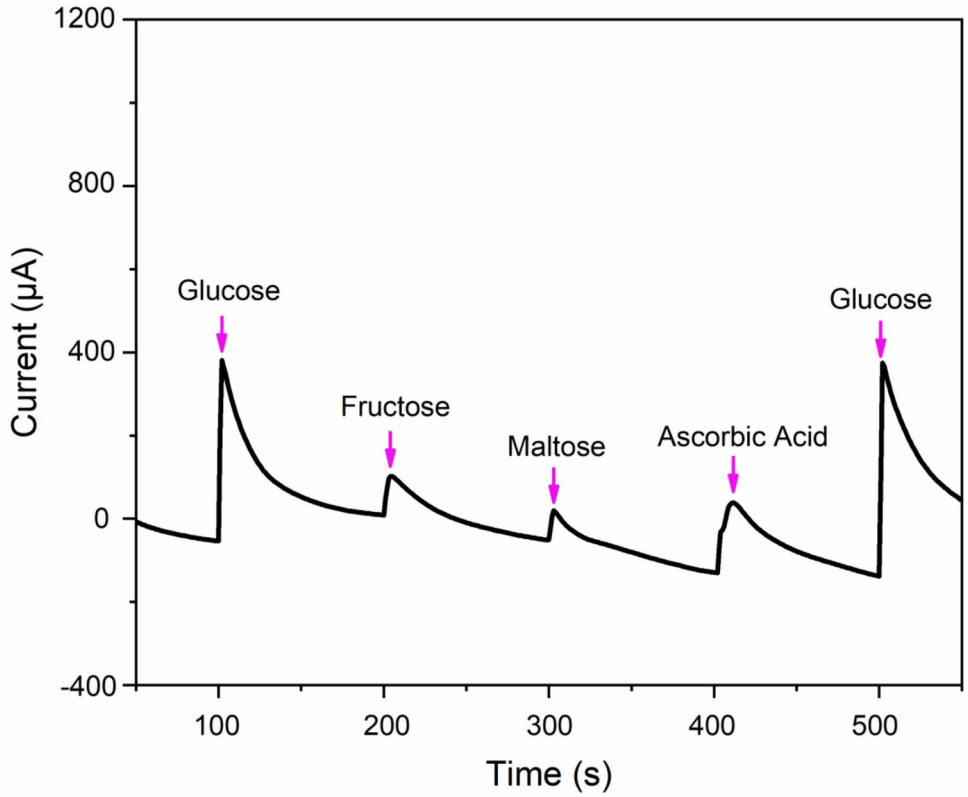


**Fig. 11** Selectivity analysis of SPGE/Ni(OH)$_2$ through CA measurement with successive additions of glucose and some interfering species

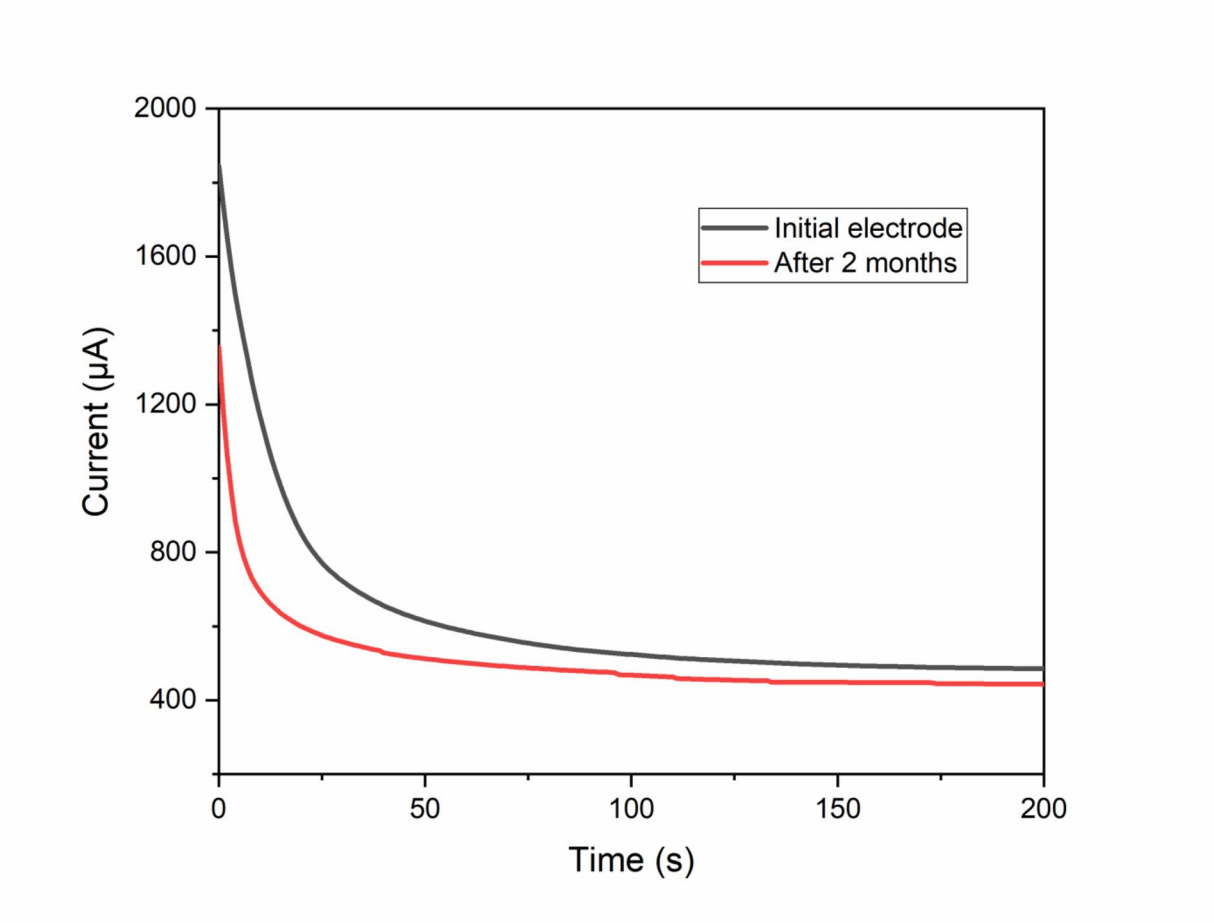


**Fig. 12** Amperometric curves recorded for 100 μM glucose by SPGE/$Ni(OH)_2$ after 2 months as compared to the initial

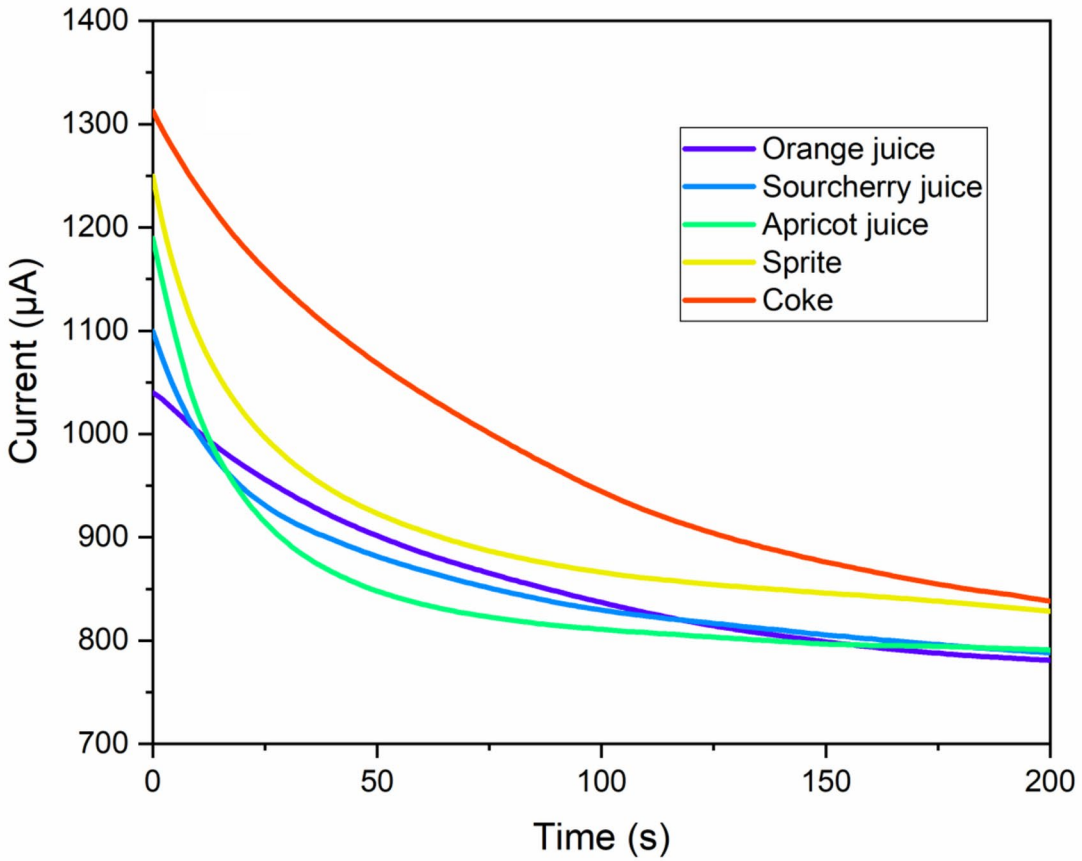


**Fig. 13** Amperometric responses of SPGE/$Ni(OH)_2$ for glucose in commercially available fluid samples of orange juice, sourcherry juice, apricot juice, sprite and coke

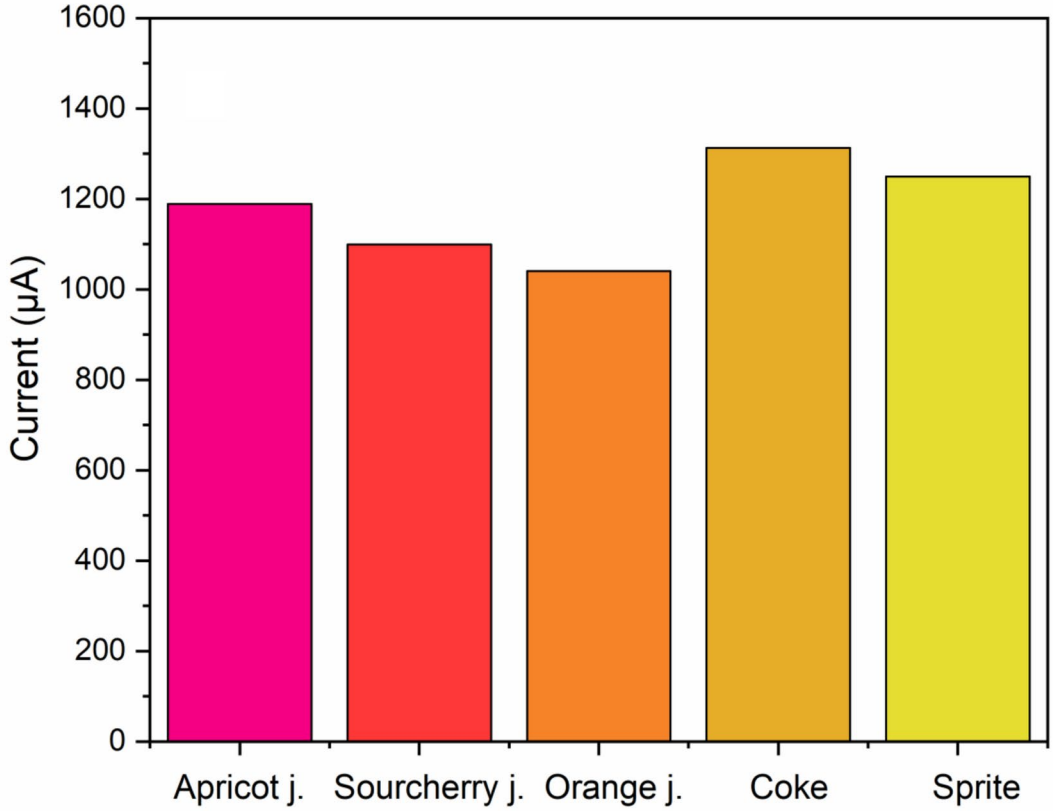


**Fig. 14** Plot of the current in real samples

**Table 1** Sugar concentration values in commercially available fluids and their corresponding current responses for the SPGE/$Ni(OH)_2$

| Fluid | Available concentration (g/mL) | Obtained response using SPGE/$Ni(OH)_2$ (μA) |
|---|---|---|
| Apricot juice | 0.064 | 1189.36 |
| Sourcherry juice | 0.060 | 1099.23 |
| Orange juice | 0.058 | 1040.17 |
| Coke | 0.106 | 1312.67 |
| Sprite | 0.09 | 1249.48 |

**Table 2** Comparison of SPGE/$Ni(OH)_2$ catalyst performance with other Ni-based glucose sensors

| Catalyst | Morphology | Electrode | Chemical Environment | Linear range | Limit of detection | Selectivity | Refs. |
|---|---|---|---|---|---|---|---|
| $Ni(OH)_2$ | Nanorod | ITO | 0.2 M NaOH | 0.1–156 mM | 70 µM | Ascorbic acid, uric acid, dopamine | [40] |
| $Ni(OH)_2$ NP/MoSx | Thin film | Glassy carbon electrode | 0.1 M KOH | 0.01–1.3 mM | 5.8 µM | Ascorbic acid, dopamine, uric acid, fructose, galactose | [41] |
| Ni/VCNTs/G | Nanotube | Graphite foil | 0.1 M NaOH | 0.05–1.0 mM | 30 µM | Ascorbic acid, uric acid, galactose, xylose | [30] |
| β-Ni $(OH)_2$/NP-Ni | Nanopetal | Metallic glass | 0.2 M NaOH | 1–18 mM | 0.35 µM | Fructose, sucrose, uric acid, ascorbic acid, NaCl | [42] |
| $Ni(OH)_2$ | Nanosheet | Polyurethane sponge | 0.1 M NaOH | 0.01–2.06 mM | 0.32 µM | Ascorbic acid, dopamine, uric acid | [43] |
| Ni/$Ni(OH)_2$/MIP | Nanoparticle | Screen printed carbon electrode | 0.1 M NaOH | 0.04–2.6 mM | 8.2 µM | Ascorbic acid, uric acid | [44] |
| CuO/$Ni(OH)_2$ | Nanosheet | Carbon cloth | 0.1 M NaOH | 0.05–8.5 mM | 0.31 µM | Ascorbic acid, dopamine, uric acid, NaCl | [45] |
| Ni/Au bilayer | Nanowire | Glassy carbon electrode | 1 M NaOH | 0.05-65 mM | 10.69 µM | NaCl, ascorbic acid, dopamine, uric acid | [46] |
| Ni-MOF/$Ni(OH)_2$ | Nanorod | Glassy carbon electrode | 0.1 M NaOH | 0.001-3.4 mM | 0.7 µM | Fructose, lactose, sucrose, ascorbic acid, dopamine, uric acid | [47] |
| $Ni(OH)_2$ | Nanoparticle | Inconel 625foam | 0.1 M NaOH | 0.001-10 mM | 2 µM | Ascorbic acid, acetaminophen, sucrose, uric acid | [48] |
| NiO | Thin film | FTO | 0.5 mM KOH | 25 µM-5 mM | 2 µM | Ascorbic acid, uric acid, folic acid, KOH | [49] |
| Ni@$Ni(OH)_2$ | Nanosheet | Glassy carbon electrode | 0.1 M NaOH | 1 µM-3.1 mM | 9.1 µM | NaCl, KCl, urea, sucrose, fructose, ascorbic acid | [50] |
| Ni-Cu alloy | Thin film | Titanium substrate | 0.1 M KOH | 0.25-8 mM | 4.97 µM | Ascorbic acid, uric acid, oxalic acid, fructose, sucrose, NaCl, $KNO_3$ | [51] |
| Ni-Niacin MOF | Nanorod | Carbon paste electrode | 0.1 M NaOH | 0.06–28.5 mM | 6 µM | Fructose, lactose, dopamine, KCl, uric acid, ascorbic acid | [52] |
| $Ni(OH)_2$ | Thin film | SPGE | 0.1 M NaOH | 0.01–0.2 mM | 1.8 µM | Ascorbic acid, fructose, maltose | This work |

**Acknowledgements** None declared.

**Author Contributions** Cigdem Dulgerbaki wrote the main manuscript text, prepared figures and reviewed the manuscript.

**Funding** Open access funding provided by the Scientific and Technological Research Council of Türkiye (TÜBİTAK).
The authors received no financial support for the research.

**Data Availability** All the data generated or analyzed in this study are included in the article file.

## Declarations

**Competing Interests** The authors declare no competing interests.



## References

1. A. Afroz, M.J. Alramadan, M.N. Hossain, L. Romero, K. Alam, D.J. Magliano, B. Billah, BMC Health Serv. Res. **18**, 1 (2018)
2. M. Lu, Y. Deng, Y. Li, T. Li, J. Xu, S.W. Chen, J. Wang, Anal. Chim. Acta. **1110**, 35 (2020)
3. W. Hu, D.W. Sun, H. Pu, T. Pan, Compr. Rev. Food Sci. Food Saf. **15**, 1067 (2016)
4. D. Arif, Z. Hussain, M. Sohail, M.A. Liaqat, M.A. Khan, T. Noor, Front. Chem. **8**, 573510 (2020)
5. S.W. Lee, T.H. Kang, S.K. Lee, K.Y. Lee, H. Yi, ACS Appl. Mater. Interfaces. **10**, 36267 (2018)
6. A.D. Daud, H.N. Lim, I. Ibrahim, N.A. Endot, N.S.K. Gowthaman, Z.T. Jiang, K.E. Cordova, J. Electroanal. Chem. **921**, 116676 (2022)
7. A.R. Abbasi, M. Yousefshahi, K. Daasbjerg, J. Inorg. Organomet. Polym. Mater. **30**, 2027 (2020)
8. R. Qin, Y. Zhou, Y. Zhao, L. Hao, J. Inorg. Organomet. Polym. Mater. **34**, 712 (2024)
9. N. Pal, B. Saha, S.K. Kundu, A. Bhaumik, S. Banerjee, New. J. Chem. **39**, 8035 (2015)
10. J. Chen, W.D. Zhang, J.S. Ye, Electrochem. Commun. **10**, 1268 (2008)
11. L.C. Jiang, W.D. Zhang, Biosens. Bioelectron. **25**, 1402 (2010)
12. X.C. Dong, H. Xu, X.W. Wang, Y.X. Huang, M.B. Chan-Park, H. Zhang, L.H. Wang, W. Huang, P. Chen, ACS Nano. **6**, 3206 (2012)
13. Y. Mu, D.L. Jia, Y.Y. He, Y.Q. Miao, H.L. Wu, Biosens. Bioelectron. **26**, 2948 (2011)
14. A. Safavi, N. Maleki, E. Farjami, Biosens. Bioelectron. **24**, 1655 (2009)
15. Y. Zhang, F.G. Xu, Y.J. Sun, Y. Shi, Z.W. Wen, Z. Li, J. Mater. Chem. **21**, 16949 (2011)
16. S. Kaneko, T. Ito, Y. Hirabayashi, T. Ozawa, T. Okuda, Y. Motoizumi, K. Hirai, Y. Naganuma, M. Soga, M. Yoshimoto, K. Suzuki, Talanta. **84**, 579 (2011)
17. P.R. Martins, M.A. Rocha, L. Angnes, H.E. Toma, K. Araki, Electroanal. **23**, 2541 (2011)
18. C.X. Wang, L.W. Yin, L.Y. Zhang, R. Gao, J. Phys. Chem. C **114**, 4408 (2010)
19. J. Ping, Y. Wang, K. Fan, J. Wu, Y. Ying, Biosens. Bioelectron. **28**, 204 (2011)
20. R.A.S. Couto, J.L.F.C. Lima, M.B. Quinaz, Talanta. **146**, 801 (2016)
21. M. Metto, S. Eramias, B. Gelagay, A.P. Washe, Int. J. Electrochem., **2019**, 6318515 (2019)
22. M. Bauer, L. Wunderlich, F. Weinzierl, Y. Lei, A. Duerkop, H.N. Alshareef, A.J. Baeumner, Anal. Bioanal Chem. **413**, 763 (2021)
23. A. Mart´ın, J. Kim, J.F. Kurniawan, J.R. Sempionatto, J.R. Moreto, G. Tang, A.S. Campbell, A. Shin, M.Y. Lee, X. Liu, J. Wang, ACS Sens. **2**, 1860 (2017)
24. N. Kusnin, N.A. Yusof, N.A.A. Mutalib, F. Mohammad, J. Abdullah, S. Sabri, S. Mustafa, A.F.M. Saman, F.N.M. Faudzi, A.A. Soleiman, Coatings. **12**, 622 (2022)
25. G.R. Fu, Z.A. Hu, L.J. Xie, X.Q. Jin, Y.L. Xie, Y.X. Wang, Z.Y. Zhang, Y.Y. Yang, H.Y. Wu, Int. J. Electrochem. Sci. **4**, 1052 (2009)
26. Y. Li, J. Yao, Y. Zhu, Z. Zou, H. Wang, J. Power Sources. **203**, 177 (2012)
27. J. Nai, S. Wang, Y. Bai, L. Guo, Small. **9**, 3147 (2013)
28. Y. Mu, D. Jia, Y. He, Y. Miao, H.-L. Wu, Biosens. Bioelectron. **26**, 2948 (2011)
29. M.A. Kiani, M. Abbasnia Tehrani, H. Sayahi, Anal. Chim. Acta. **839**, 26 (2014)
30. W.-S. Kim, G.-J. Lee, J.-H. Ryu, K.-C. Park, H.-K. Park, RSC Adv. **4**, 48310 (2014)
31. C.-W. Kung, Y.-H. Cheng, K.C. Ho, Sens. Actuators B **204**, 159 (2014)
32. J. Yang, M. Cho, C. Pang, Y. Lee, Sens. Actuators B **211**, 93 (2015)
33. K.K. Naik, A. Gangan, B. Chakraborty, S.K. Nayak, C.S. Rout, ACS Appl. Mater. Interfaces. **9**, 23894 (2017)
34. J. Wang, D.F. Thomas, A. Chen, Anal. Chem. **80**, 997 (2008)
35. R. Kaur, S. Rana, K. Lalit, P. Singh, K. Kaur, Biosens. Bioelectron. **167**, 112486 (2020)
36. S. Chaiyo, E. Mehmeti, W. Siangproh, T.L. Hoange, H.P. Nguyene, O. Chailapakul, K. Kalcher, Biosens. Bioelectron. **102**, 113 (2018)
37. A. Sanati, E. Bidram, A. Poursamar, M. Rabbani, M. Rafienia, FlatChem. **36**, 100443 (2022)
38. R. Ahmad, N. Tripathy, M.S. Ahn, K.S. Bhat, T. Mahmoudi, Y. Wang, J.Y. Yoo, D.W. Kwon, H.Y. Yang, H.B. Hahn, Sci. Rep. **7**, 5715 (2017)
39. S.A. Shabbir, S. Tariq, M. Gul Bahar, W.A. Ashiq, Khan, Biosci. Rep. **39**, 1 (2019)
40. N. Pal, S. Banerjee, A. Bhaumik, J. Colloid Interface Sci. **516**, 121 (2018)
41. S. Ji, Z. Yang, C. Zhang, Y.-E. Miao, W.W. Tjiu, J. Pan, T. Liu, Microchim Acta. **180**, 1127 (2013)
42. Y. Zhang, D. Zheng, S. Liu, S. Qin, X. Sun, Z. Wang, C. Qin, Y. Li, J. Zhou, Appl. Surf. Sci. **552**, 149529 (2021)
43. S. Guo, C. Zhang, M. Yang, Y. Zhou, C. Bi, Q. Lv, N. Ma, Anal. Chim. Acta. **1109**, 130 (2020)
44. R. Sylvain, G. Dykstra, A. Fungura, S. Rao, Y. Liu, Sens. Actuators: B Chem. **424**, 136921 (2025)
45. S. Sun, N. Shi, X. Liao, B. Zhang, G. Yin, Z. Huang, X. Chen, X. Pu, Appl. Surf. Sci. **529**, 147067 (2020)

46. M. Wang, F. Liu, M. Shi, F. Gong, F. Li, J. Electron. Mater. **51**, 2490 (2022)
47. L. Xiao, X. Fang, Y. Cao, L. Hu, J. Jiang, Microchem J. **190**, 108694 (2023)
48. R. Kihal, H. Fisli, M.L. Chelaghmia, W. Drissi, C. Boukharouba, S. Abdi, M. Nacef, A.M. Affoune, M. Pontié, J. Appl. Electrochem. **53**, 315 (2023)
49. D.K. Pathak, H.C. Moon, Mater. Des. **234**, 112309 (2023)
50. P. Pathmanathan, A. Gomathi, A. Ramesh, Ch Subrahmanyam RSC Adv. **14**, 21808 (2024)
51. K. Hebbache, N.A. Ahmed, N. Aliouane, M. Eyraud, K. Mira, A. Achouri, A. Djermoune, Ionics. **30**, 3455 (2024)
52. A. Afruz, M. Amiri, M. Kaffash-Jamshid, A. Bezaatpour, P. Bottke, M. Wark, Electrochim. Acta. **513**, 145586 (2025)